

Design of a five-dimensional fractional-order chaotic system and its sliding mode control

Y Tong^{1*} , Z Cao¹, H Yang¹, C Li² and W Yu³

¹School of Information Science and Engineering, Hunan Institute of Science and Technology, Yueyang 414006, Hunan, China

²School of Physics and Electronics, Hunan Institute of Science and Technology, Yueyang 414006, Hunan, China

³School of Information and Electrical Engineering, Hunan University of Science and Technology, Xiangtan 411201, Hunan, China

Received: 22 February 2021 / Accepted: 09 July 2021 / Published online: 12 August 2021

Abstract: The movement presented by chaos is violent oscillation, making the system unstable, which often is harmful in engineering. Therefore, how to suppress chaotic state quickly is a research hotspot in the field of control. Compared with integer-order system, fractional-order chaotic system has more complex dynamic characteristics, and it is often difficult to control the dynamic system into a stable periodic motion. In this paper, a new sliding mode controller was proposed after newly constructing a fractional-order chaotic system, to make the chaotic system enter a predetermined motion state quickly and maintain stability. Firstly, a new five-dimensional fractional-order chaotic system was constructed, analyzing its dynamic characteristics through the 0–1 test. Then, a sliding mode controller was designed, with proved stability to regulate the motion state of chaotic system. Finally, the circuit realization and control process simulation of the five-dimensional fractional-order chaotic system were carried out. The experimental results show that the proposed sliding mode controller has simple structure, but fast response and excellent control effect.

Keywords: Fractional order; Chaos; Circuit; Sliding mode control

1. Introduction

Chaos is one of the greatest discoveries in physics in the twentieth century, after relativity and quantum mechanics [1]. Chaos control, as an important part of chaos theory, has become a research hotspot nowadays because of its great application value in the field of engineering technology [2–9]. For secure communication, signal processing and system control, compared with the integer-order system, the fractional-order chaotic system has more prominent application prospects, which, therefore, has received much attention in the research. Previous studies have found the facts that fractional-order chaotic systems are more accurate than integer-order systems, with long history in its calculus theory, which is the same as that of integer-order system, but develops slower due to its lack of application background. Up to now, although a lot of work has been conducted in the field of fractional-order calculus, the research on revealing the relationship between fractal,

chaos and fractional-order systems has just started, including fractional-order chaos and hyperchaos, fractional-order chaos control and synchronization, the realization and application of fractional-order chaotic systems, etc.

When chaos appears in some systems, continuous irregular oscillations will occur along with the system operation, which seriously endangers the safe operation of the system. For example, if there is chaos in the power system, the operating parameters will oscillate irregularly and continuously, which may cause system instability of the system and endanger its safe operation seriously. When permanent magnet synchronous motor (PMSM) appears chaotic motion under certain working conditions, it may have violent oscillation of speed or torque, unstable control performance and irregular electromagnetic noise, etc. Brushless direct current motor (BLDCM) will produce nonlinear chaotic motion during operation, resulting in torque pulsation. There is also chaotic phenomena in the switching circuit, which although does not cause destructive harm in switching converters, but is still unstable for communication power systems requiring high reliability.

*Corresponding author, E-mail: tongyaon@hnist.edu.cn

Chaos in the circuit system will destroy its stability and harm the circuit components. Therefore, it is of great significance to control the chaos in the system, even suppress its generation.

At present, the research on chaos control is mainly from two aspects. One is chaos control and synchronization, which means that when the chaos already exists and is disadvantageous to the movement of the system or leads to an unfavorable trend, it is necessary to control the chaotic system by specific methods to weaken or eliminate the harm of chaos. The other is the anti-control of chaos, which aims to selectively produce or maintain and strengthen the already generated chaotic state. In the field of integer order, nonlinear system control based on Lyapunov stability theory has been extensively studied, with a series of results [10–14]. However, due to the late start of fractional-order control and its complexity, the theory of fractional-order stability and controller design methods is far inferior to those of integer-order system. The current control methods for fractional-order chaotic systems include linear feedback, impulse control, adaptive control method, etc. In practical applications, there are often modeling errors, measurement errors, structural changes, environmental noise and other factors, which can cause uncertainty and external interference that are inevitable. Therefore, it is of great practical significance to study fractional-order chaotic system. In [15], a fractional-order unstable dissipative system was introduced and analyzed. Chaos with different fractional orders was observed as a function of the system's parameters. Furthermore, the topological horseshoe for lower fractional orders was found. In [16], a new unbalanced dynamic system with multi-volume attractors was proposed, which was a piecewise linear system, simple, stable, showing chaos, and similar to a nonlinear system. In [17], a dynamic system based on the Langevin equation was proposed, with no random terms, representing the properties of Brownian motion with fractional derivatives. In [18], the electronic implementation of a fractional Rössler system with an operational transconductance amplifier was introduced, with the advantages of low voltage realization, integration and electronic adjustability. In [19], a new fractional four-dimensional system was proposed, exhibiting some hidden hyperchaotic attractors.

Sliding mode variable structure control [20–23] is a special nonlinear control strategy, which can change constantly according to the current state, so as to force the system to move according to a predetermined sliding mode state trajectory. In [24], a sliding mode hyperplane was designed for a class of chaotic systems with uncertainties. A new method of composite sliding mode control for a class of uncertain chaotic systems was proposed in the literature [25]. In [26], a nonlinear sliding mode controller was proposed and applied to the nonlinear chaotic system. In [27], the sliding mode control for a class of fractional-

order chaotic systems was studied, which could ensure the asymptotic stability of uncertain fractional-order chaotic systems in the presence of external disturbances. The literature [28] proposed a switching sliding mode control technique for chaos control and suppression of non-autonomous fractional-order nonlinear power systems with uncertainties and external disturbances. All the above researches have made important contributions to the development of chaos control theory.

In this paper, a new sliding mode controller was proposed for a new five-dimensional fractional-order chaotic system, making the chaotic system enter a predetermined stable motion state quickly. The structure of this paper is as follows. In the second part, a five-dimensional fractional-order chaotic system was constructed, and then its dynamics was analyzed through 0–1 test. In order to realize the state control, a sliding mode controller was designed in the third part, and its stability was proved to effectively suppress the chaos. In the experimental part, circuit realization and control process simulation of the five-dimensional fractional-order chaotic system were carried out, respectively.

2. Construction and dynamics analysis of the new chaotic system

In this section, definition of fractional differential equation was presented firstly. Caputo derivative of fractional order α of function $x(t)$ is defined as follows:

$$D_{t_0}^q = J_{t_0}^{m-q} D_{t_0}^m x(t) = \begin{cases} \frac{1}{\Gamma(m-q)} \int_{t_0}^t (t-\tau)^{m-q-1} x^{(m)}(\tau) d\tau \\ \frac{d^m x(t)}{dt^m}, \quad q = m \end{cases} \quad (1)$$

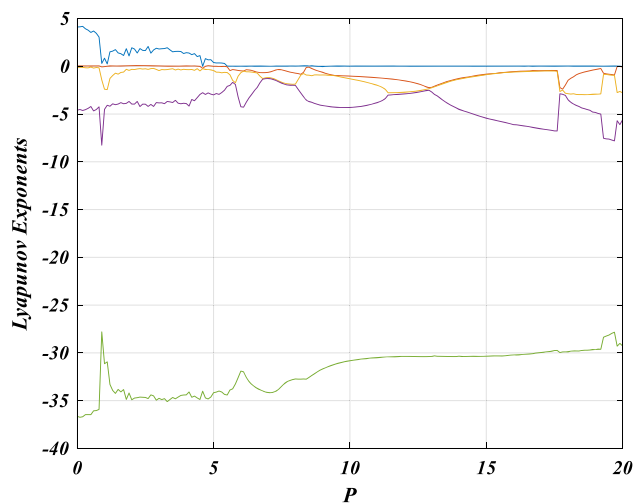


Fig. 1 Lyapunov exponent spectra

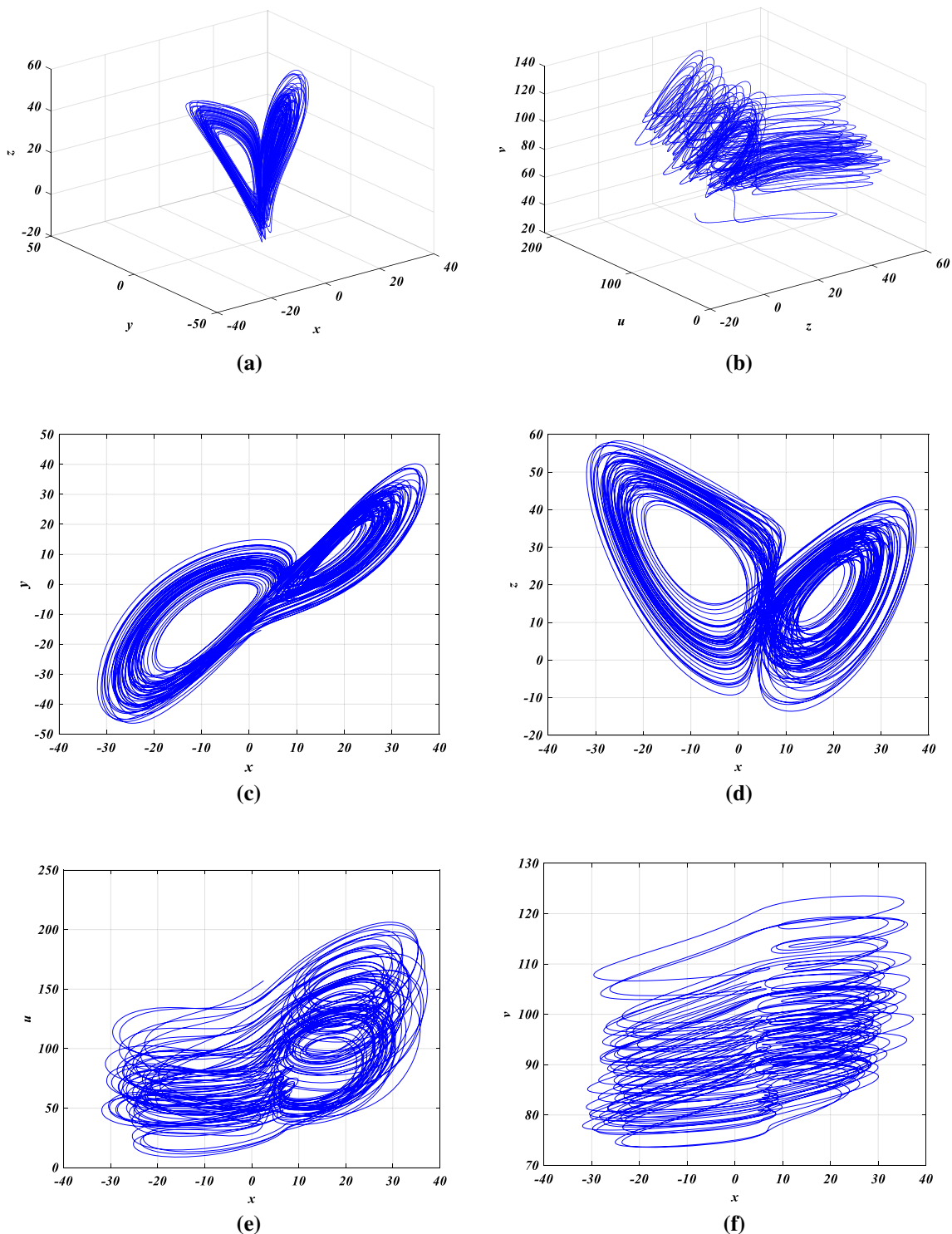


Fig. 2 Projections of attractor onto different planes of a five-dimensional fractional-order system

where $m - 1 < q < m \in \mathbb{Z}^+$, the operator $D_{t_0}^q$ is the Caputo fractional differential operator of order q , $\Gamma(\bullet)$ is the Gamma function. For the convenience of writing this paper, $D_{t_0}^q$ is replaced by $\frac{d^q}{dt^q}$.

2.1. System modeling

In this paper, a new five-dimensional fractional-order chaotic system was designed as follows:

$$\begin{cases} \frac{d^\alpha x}{dt^\alpha} = 30(y - x) + u + 2v - 5z \\ \frac{d^\beta y}{dt^\beta} = 10x - xz + 12y \\ \frac{d^\gamma z}{dt^\gamma} = xy - 3z - v - 4x \\ \frac{d^\delta u}{dt^\delta} = pxy + yz - 2u \\ \frac{d^\epsilon v}{dt^\epsilon} = 3y \end{cases} \quad (2)$$

For systems with dimensionality greater than 1, there exists a set of Lyapunov exponents, commonly known as the Lyapunov exponent spectrum, where each of them characterizes the convergence of the orbit in a certain direction. Lyapunov exponent, a quantitative description of the long-term average result of orbital exponent separation of the system, is an overall characteristic of the system, with a wide range of values which have no effect on the system state. The state of the system is determined primarily by positive and negative values of all Lyapunov exponents. When the value of Lyapunov exponent is positive, each part of the trajectory is unstable, and adjacent trajectories repel each other, separating rapidly at exponential speed, producing chaotic attractors with specific patterns. When the value of Lyapunov exponent is 0, it lies on the boundary of the relatively stable trajectory. When the value of Lyapunov exponent is negative, the phase volume shrinks, with the locally stable trajectory, corresponding to the periodic orbital motion. Therefore, it can be judged whether the system is in a chaotic state according to the values of Lyapunov exponent.

Suppose five Lyapunov exponents are $\lambda_i (i = 1, 2, 3, 4, 5)$. According to the theory of Lyapunov exponent spectrum, we have $\lambda_5 < \lambda_4 < \lambda_3 < \lambda_2 < \lambda_1 < 0$ for equilibrium points; $\lambda_1 = 0, \lambda_5 < \lambda_4 < \lambda_3 < \lambda_2 < 0$ for periodic states; $\lambda_1 = \lambda_2 = 0, \lambda_5 < \lambda_4 < \lambda_3 < 0$ for pseudo-periodic states; and $\lambda_1 > \lambda_2 = 0, \lambda_5 < \lambda_4 < \lambda_3 < 0, \lambda_1 + \lambda_3 + \lambda_4 + \lambda_5 < 0$ for chaotic states. From Fig. 1, $P \in [0, 5.5]$, $\lambda_1 > \lambda_2 = 0, \lambda_5 < \lambda_4 < \lambda_3 < 0, \lambda_1 + \lambda_3 + \lambda_4 + \lambda_5 < 0$ is for a chaotic state, and $P \in [5.5, 20]$, $\lambda_1 = 0, \lambda_5 < \lambda_4 < \lambda_3 < \lambda_2 < 0$ is for a periodic state.

When the system parameter $p = 1$, projections of attractor onto different planes for the designed five-dimensional fractional-order chaotic system are shown in Fig. 2.

2.2. Dynamics analysis

At present, the commonly used methods for chaos identification mainly include phase diagram method, Poincaré mapping method, spectrum analysis method, and Lyapunov exponent method, with certain adaptability, but limitations. For example, phase diagram method is simple and intuitive, but its accuracy is not high enough. Poincaré mapping method cannot directly distinguish between chaotic and completely random motions. The calculation results of the maximum Lyapunov exponent method were not

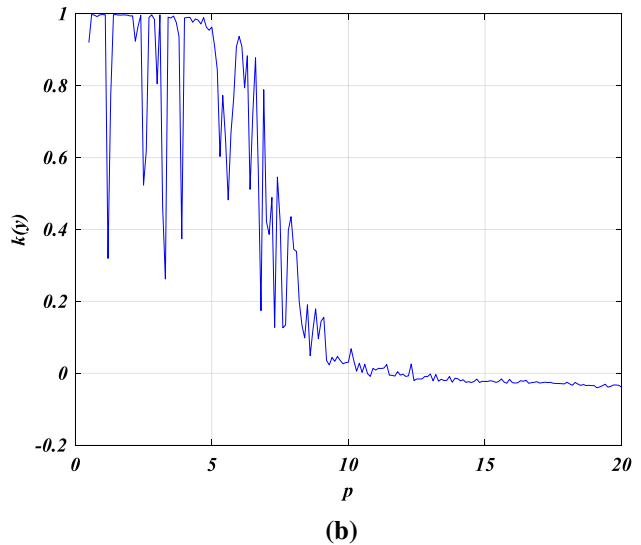
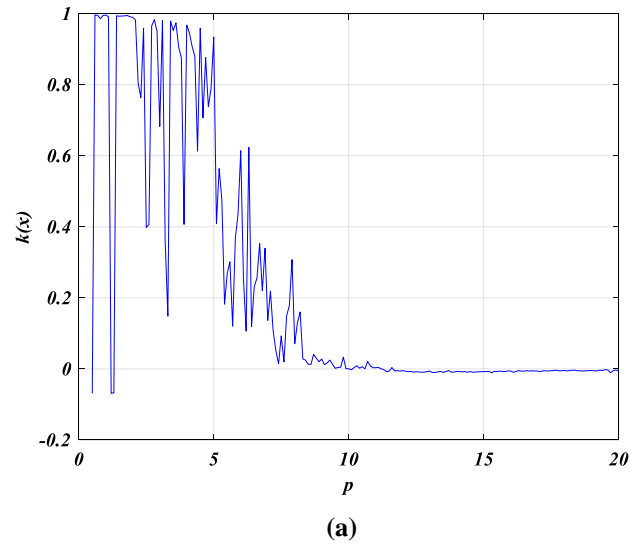


Fig. 3 Changes of median values of asynchronous growth rate k with parameter p

directly obtained in this paper. The determination of delay time and embedding dimension has certain subjectivity and uncertainty.

Gottwald GA and Melbourne I [29] proposed a reliable and effective binary method for testing the chaos in the system, which is called the “0–1 test”. A discrete set $\{(j)\} (j = 1, 2, \dots, N)$ was formed with any positive number $c \in [\pi/5, 4\pi/5] > 0$ and numerical simulation data. When n does not exceed 0.1 times of N , the conversion variables can be defined as follows:

$$p_c(n) = \sum_{i=1}^n \phi(i) \cos ic, \quad q_c(n) = \sum_{i=1}^n \phi(i) \sin ic$$

In order to quantify the growth features (such as diffusion behavior) of the characterization functions $p_c(n)$

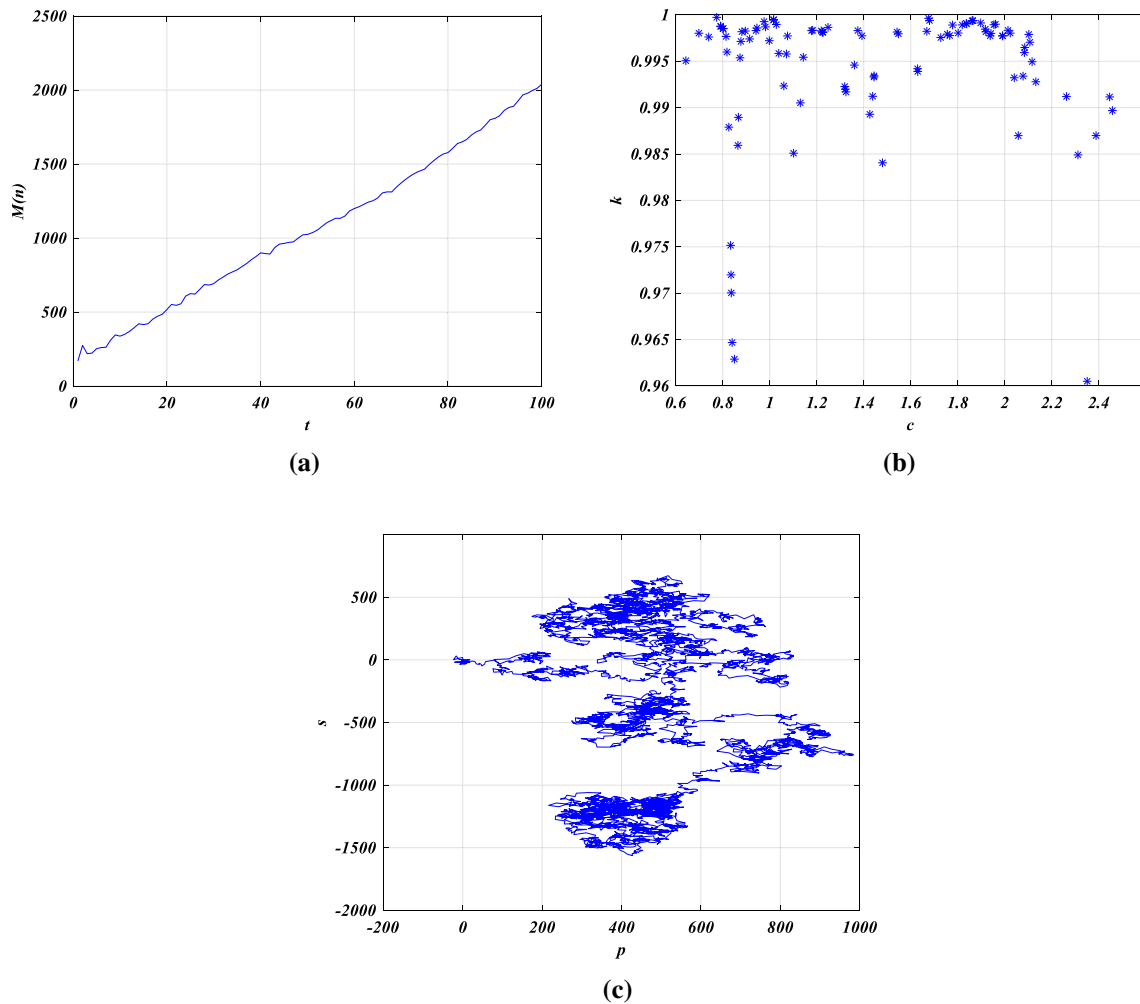


Fig. 4 Test results of system 0-1 test with $p = 1$

and $q_c(n)$, the mean square displacement (MSD) of $p_c(n)$ and $q_c(n)$ is defined as follows:

$$M_c(n) = \lim_{N \rightarrow \infty} \left\{ \sum_{i=1}^N [p_c(i+n) - p_c(i)]^2 + [q_c(i+n) - q_c(i)]^2 \right\} - \left[\lim_{N \rightarrow \infty} \frac{1}{N} \sum_{i=1}^N \Phi(i) \right]^2 \frac{1 - \cos nc}{1 - \cos c}$$

The convergence and divergence of functions $p_c(n) - q_c(n)$ can be directly measured by $M_c(n)$. The asymptotic growth rate K_c of $M_c(n)$, the characteristic index of chaos for dynamic system, can be obtained by linear regression fitting $\log M_c(n)$ and $\log n$, which can also be replaced by the correlation coefficient of the two.

Specific steps of the algorithm are as follows:

- 1) Use the first data point N of different fractional-order chaotic systems as a discrete set $\Phi(N)$;
- 2) Take one data point from every 8 data points to replace the discrete set $\Phi(N)$;

- 3) Substitute $\Phi(N)$ into the conversion variable to get $p_c(n) - q_c(n)$, and display them in the form of trajectory image $p_c(n) - q_c(n)$;
- 4) The image of MSD $M_c(n)$ varying with n and the progressive growth rate K_c of $M_c(n)$, derived from $p_c(n) - q_c(n)$;
- 5) Take the Median of all K_c as median value of K_c . The discrete set $\Phi(N)$ shows chaotic characteristics. When K_c tends to 1 and 0, the discrete set $\Phi(N)$ shows non-chaotic characteristics.

The following judgment rules were adopted: if $p_c(n) - q_c(n)$ presents the form of random Brownian motion, $M_c(n)$ increases linearly with the time evolution, and K_c is close to 1, then the sequence is judged to be a chaotic time sequences. If $p_c(n) - q_c(n)$ graph presents a bounded periodic ring, $M_c(n)$ is bounded, and K_c is close to 0, then it is judged to be a non-chaotic time sequences (periodic or period-doubling). Because the parameter c may have a frequency resonance effect with the Fourier decomposition

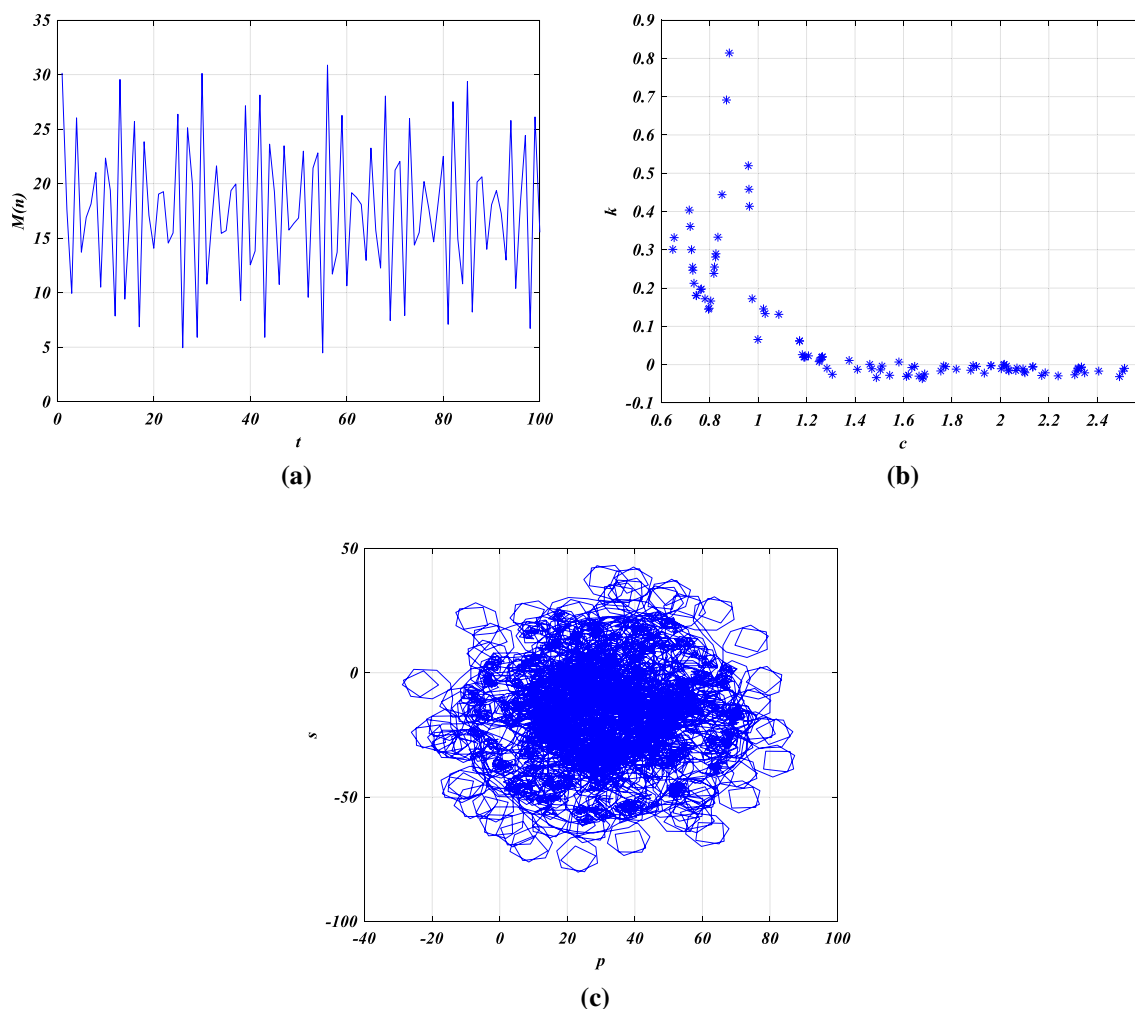


Fig. 5 Test results of system 0–1 test with $p = 18$

of the time series in the calculation process, the c is limited to 100 random numbers between $\pi/4$ and $4\pi/5$, and the final return value is the median of K_c .

The system x-dimension and y-dimension median k value changes with the system parameter p as shown in Fig. 3.

It can be seen from Fig. 3 that, when $p \in [1, 5]$, the median value k is close to 1, so the system is in a chaotic state, the system dynamics behavior is complex; when $p \in (5, 10]$, the median value k changes between 0–1, the system is in a transitional state; when $p \in [10, 20)$, the median value k is close to 0, the system is in a periodic state.

When $p = 1$, the 0–1 test result is shown in Fig. 4. It can be seen from Fig. 4 that the $p_c(n) - q_c(n)$ graph is a random Brownian motion, $M(n)$ evolves linearly with time, K_c is close to 1, and the median is calculated to be 0.9952 (which can be regarded as 1).

When $p = 18$, the 0–1 test result is shown in Fig. 5. It is shown in Fig. 5 that the $p_c(n) - q_c(n)$ graph is a periodic

ring, $M_c(n)$ is bounded, K_c is close to 0, and the median is -0.0067 (which can be regarded as 0).

3. Sliding mode controller design

The dynamic characteristics of the fractional-order system are more complex, and the stable periodic motion often lacks flexibility when controlling the dynamic system. The control of the sliding mode system has obvious advantages in this aspect. It can be adjusted by the dynamic behavior of the system. There is no need to greatly disturb and change the system to make the system operate stably on the expected orbit. Combining Eq. (2) with sliding mode control theory, we can get Eq. (3) as follows:

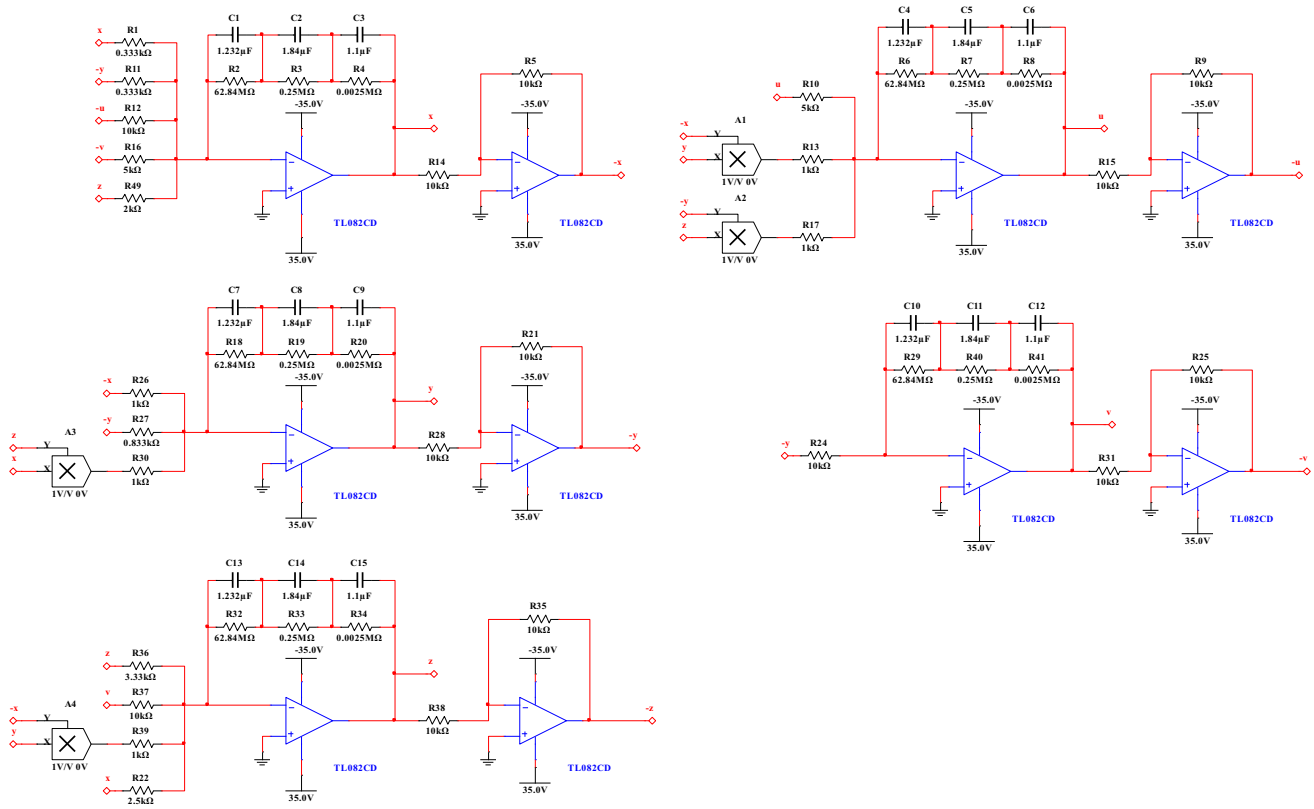


Fig. 6 Five-dimensional fractional-order chaotic system circuit (drive system)

$$\begin{cases} \frac{d^\alpha x}{dt^\alpha} = 30(y-x) + u + 2v - 5z + \delta_1 \\ \frac{d^\beta y}{dt^\beta} = 10x - xz + 12y + \delta_2 \\ \frac{d^\gamma z}{dt^\gamma} = xy - 3z - v - 4x + \delta_3 \\ \frac{d^\delta u}{dt^\delta} = xy + yz - 2u + \delta_4 \\ \frac{d^\epsilon v}{dt^\epsilon} = 3y + \delta_5 \end{cases} \quad (3)$$

And $\delta = [\delta_1 \delta_2 \delta_3 \delta_4 \delta_5]^T$ is the added sliding mode control rate corresponding to each dimension, respectively.

Suppose the sliding mode switching function of this system is as follows:

$$s = c_1 \cdot e + D_t^{-\sigma} e \quad (4)$$

where c_1 is the sliding mode parameter and $D_t^{-\sigma} e$ is the negative σ th derivative of e . And among them,

$$\begin{aligned} D_t^{-\sigma} e &= [D_t^{-\sigma} e_1 \quad D_t^{-\sigma} e_2 \quad D_t^{-\sigma} e_3 \quad D_t^{-\sigma} e_4 \quad D_t^{-\sigma} e_5]^T, \\ s &= [s_1 \quad s_2 \quad s_3 \quad s_4 \quad s_5]^T, \\ e &= [e_1 \quad e_2 \quad e_3 \quad e_4 \quad e_5] \\ &= [x - x_{ref} \quad y - y_{ref} \quad z - z_{ref} \quad u - u_{ref} \quad v - v_{ref}]^T, \end{aligned}$$

where $x_{ref}, y_{ref}, z_{ref}, u_{ref}, v_{ref}$ are reference values of state variables.

Deriving from Eq. (4) leads to Eq. (5):

$$\dot{s} = c_1 \cdot \dot{e} + D_t^{1-\sigma} e \quad (5)$$

When the parameter is $\sigma = [0.1 \ 0.1 \ 0.1 \ 0.1 \ 0.1]$, and the sliding mode reaching law is set as follows:

$$\dot{s} = -ks^3 - \varepsilon \frac{|s|^{\frac{1}{2}}}{1+|s|^2} \text{sgn}(s),$$

the control rate of sliding mode control system can be obtained by combining Eq. (4) as follows:

$$\begin{cases} \delta_1 = -ks_1^3 - \varepsilon |s_1|^{\frac{1}{2}} \text{sgn}(s_1) - c_1 \cdot D_t^1 e_1 + D_t^{0.9} x_e - 30(y-x) - u - 2v + 5z \\ \delta_2 = -ks_2^3 - \varepsilon |s_2|^{\frac{1}{2}} \text{sgn}(s_2) - c_1 \cdot D_t^1 e_2 + D_t^{0.9} y_e - 10x + xz - 12y \\ \delta_3 = -ks_3^3 - \varepsilon |s_3|^{\frac{1}{2}} \text{sgn}(s_3) - c_1 \cdot D_t^1 e_3 + D_t^{0.9} z_e - y + 3z + v + 4x \\ \delta_4 = -ks_4^3 - \varepsilon |s_4|^{\frac{1}{2}} \text{sgn}(s_4) - c_1 \cdot D_t^1 e_4 + D_t^{0.9} u_e - xy - yz + 2u \\ \delta_5 = -ks_5^3 - \varepsilon |s_5|^{\frac{1}{2}} \text{sgn}(s_5) - c_1 \cdot D_t^1 e_5 + D_t^{0.9} v_e - 3y \end{cases} \quad (6)$$

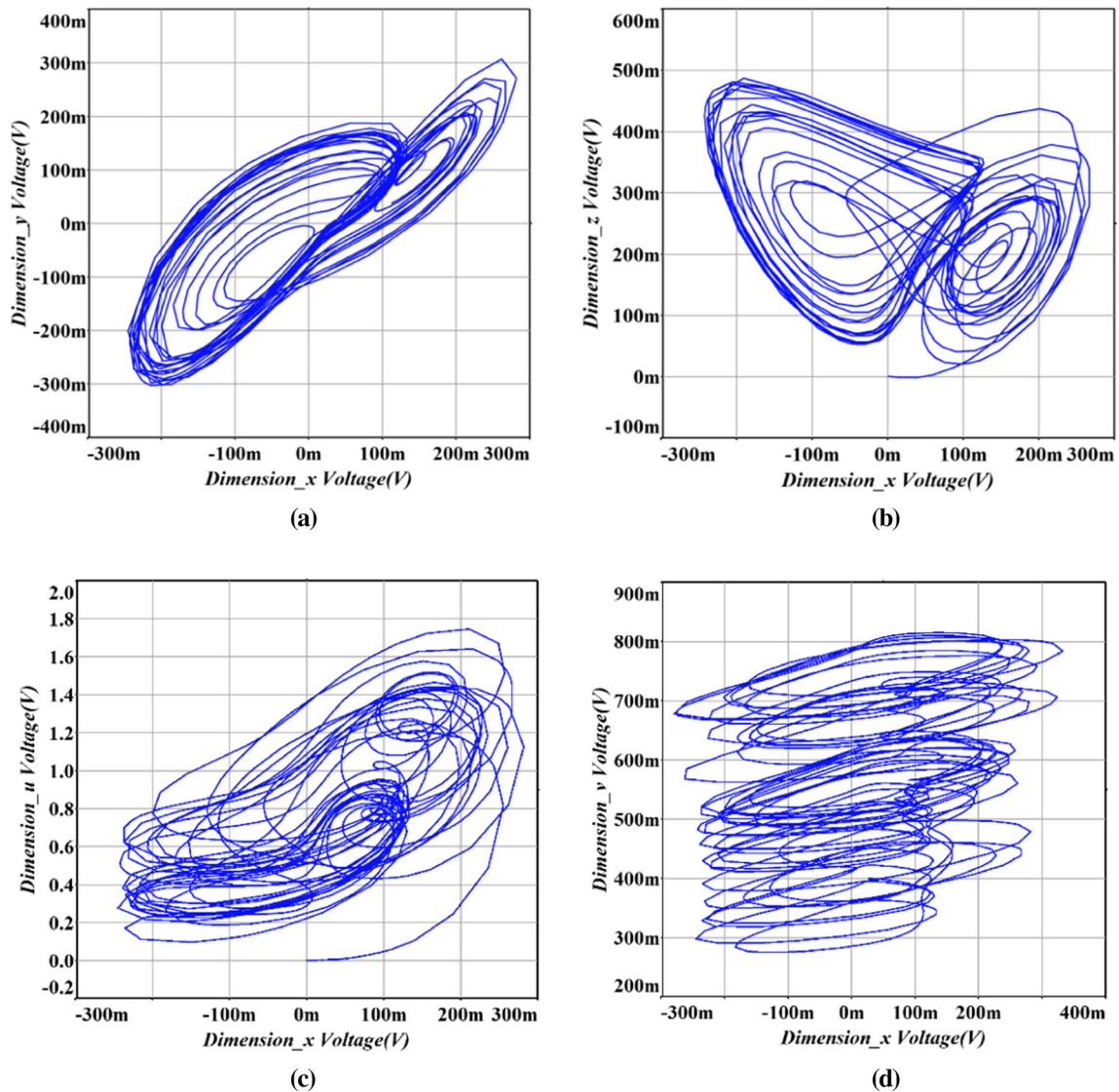


Fig. 7 MULTISIM simulation results

Proof of stability: When the Lyapunov stability theorem is satisfied, the trajectory of the system state variable will reach the sliding surface within a finite time to achieve system stability, which can prove that the system is asymptotically stable. This paper only proves the stability of the new approach rate.

Theorem 1: For a sliding mode variable structure control system, its switching function is shown in Eq. (3), and its Lyapunov function is defined as: $V = s^T \cdot s$. If $\dot{V} = s^T \dot{s} + \dot{s}^T s \leq 0$, then this control system is progressively stable.

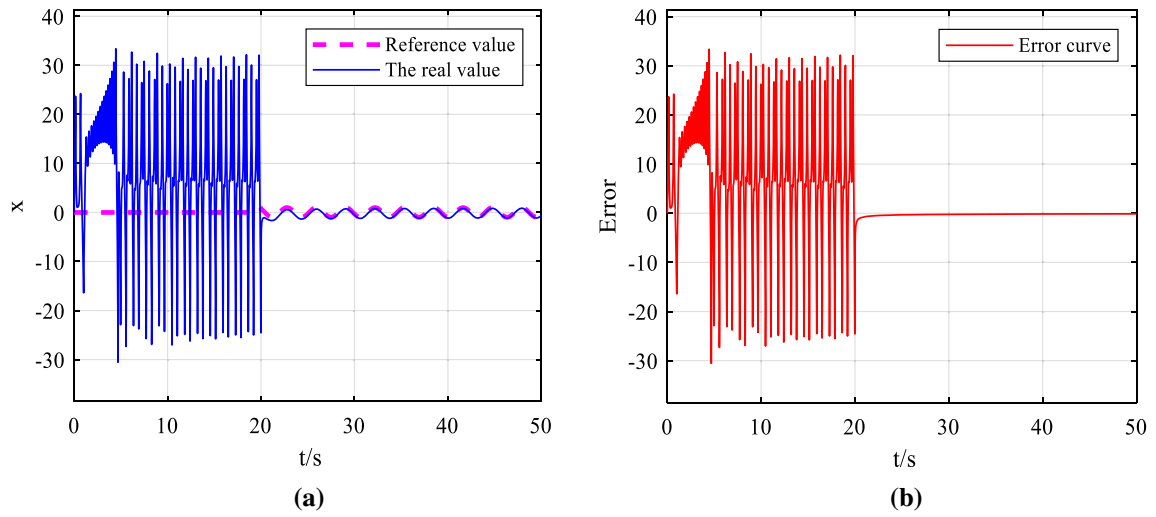


Fig. 8 x-dimensional time series and error response diagram

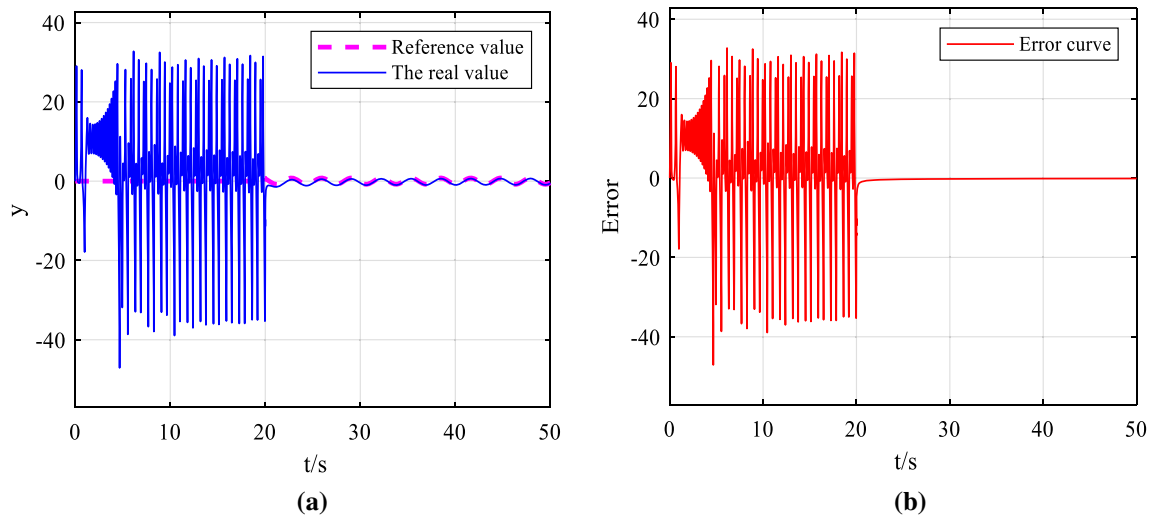


Fig. 9 y-dimensional time series and error response diagram

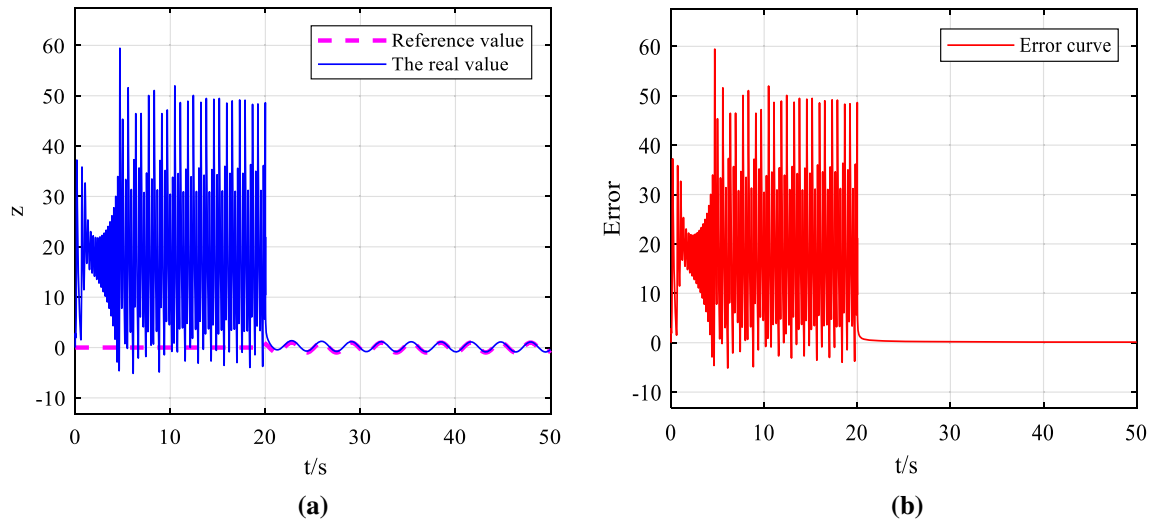


Fig. 10 z-dimensional time series and error response diagram

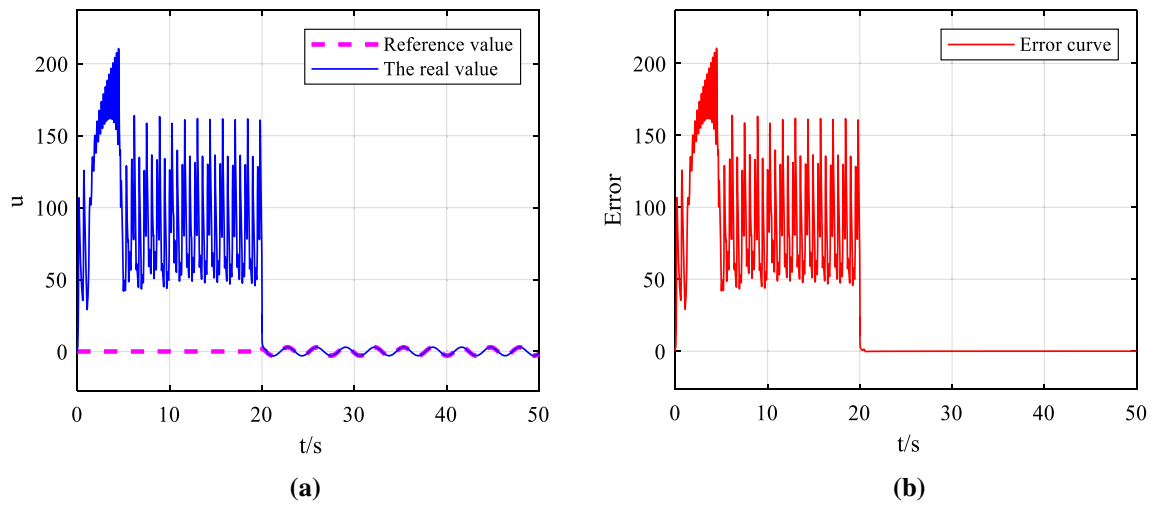


Fig. 11 u-dimensional time series and error response diagram

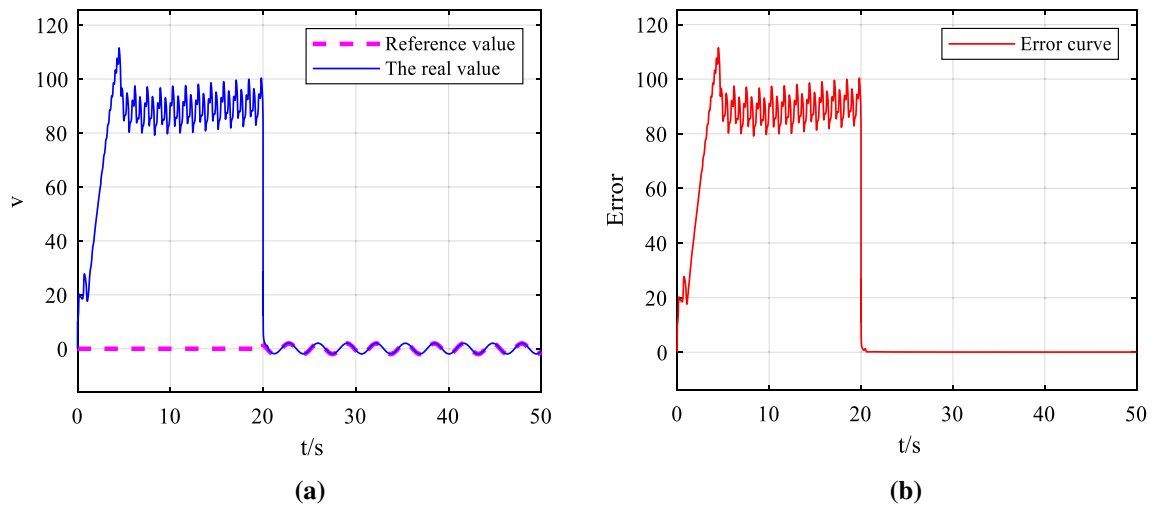


Fig. 12 v-dimensional time series and error response diagram

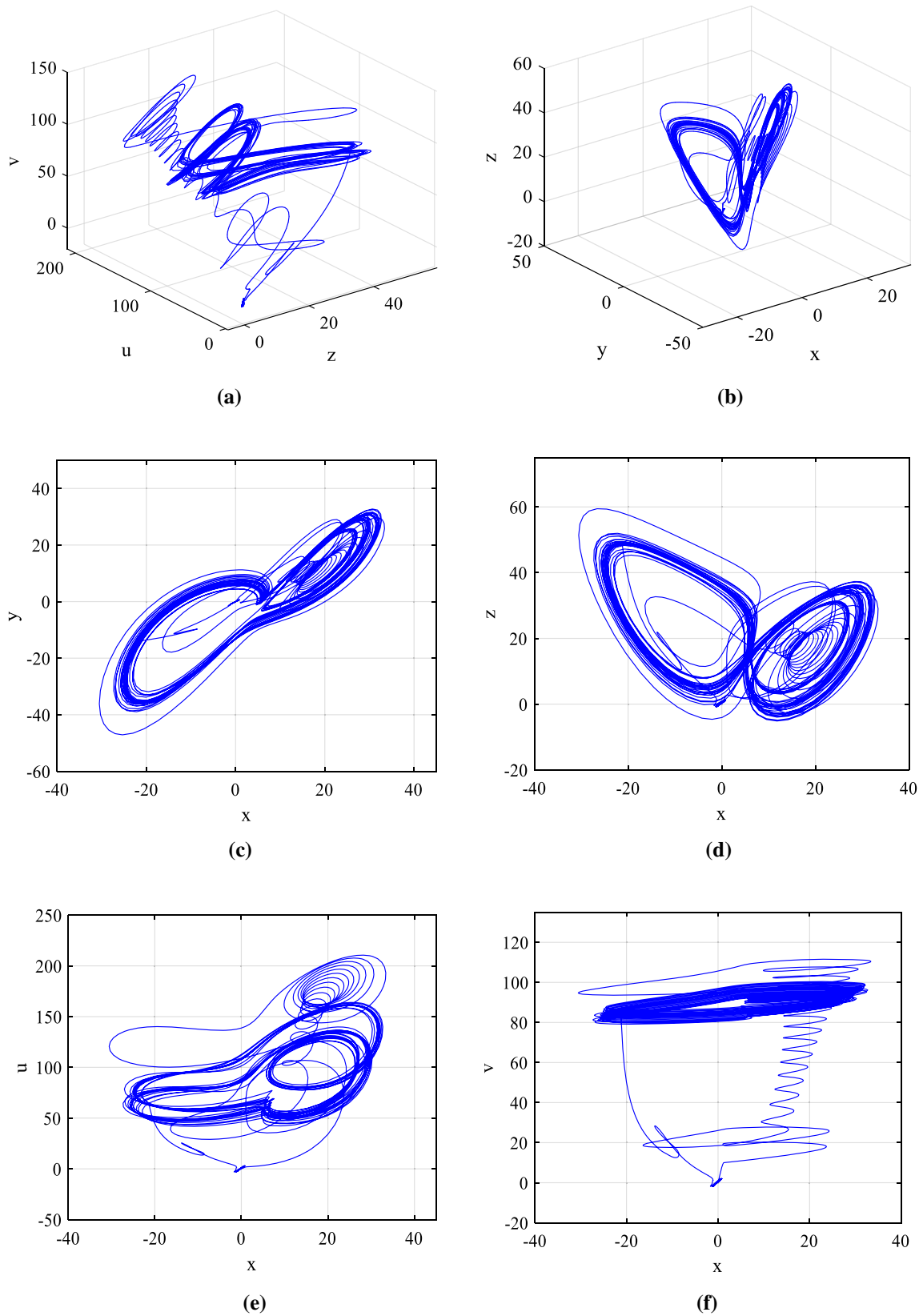


Fig. 13 Phase diagrams of a five-dimensional fractional-order system after sliding mode control

Proof:

$$\begin{aligned}
 \dot{V} &= s^T \dot{s} + s^T \dot{s} \\
 &= 2s^T \cdot \dot{s} \\
 &= 2s^T \cdot (c_1 \cdot e + D_t^{1-\sigma} e) \\
 &= 2s^T \cdot \begin{bmatrix} c_1 \cdot D_t^1 e - D_t^{0.9} x_e + 30(y-x) + u + 2v - 5z + \delta_1 \\ c_1 \cdot D_t^1 e - D_t^{0.9} y_e + 10x - xz + 12y + \delta_2 \\ c_1 \cdot D_t^1 e - D_t^{0.9} z_e + xy - 3z - v - 4x + \delta_3 \\ c_1 \cdot D_t^1 e - D_t^{0.9} u_e + xy + yz - 2u + \delta_4 \\ c_1 \cdot D_t^1 e - D_t^{0.9} v_e + 3y + \delta_5 \end{bmatrix} \\
 &= 2s^T \cdot \begin{pmatrix} ks_1^3 + e \frac{|s_1|^{\frac{1}{2}}}{1 + |s_1|^{\frac{1}{2}}} \text{sgn}(s_1) \\ ks_2^3 + e \frac{|s_2|^{\frac{1}{2}}}{1 + |s_2|^{\frac{1}{2}}} \text{sgn}(s_2) \\ ks_3^3 + e \frac{|s_3|^{\frac{1}{2}}}{1 + |s_3|^{\frac{1}{2}}} \text{sgn}(s_3) \\ ks_4^3 + e \frac{|s_4|^{\frac{1}{2}}}{1 + |s_4|^{\frac{1}{2}}} \text{sgn}(s_4) \\ ks_5^3 + e \frac{|s_5|^{\frac{1}{2}}}{1 + |s_5|^{\frac{1}{2}}} \text{sgn}(s_5) \end{pmatrix} \\
 &= -2 \left(ks_1^4 + e \frac{|s_1|^{\frac{3}{2}}}{1 + |s_1|^{\frac{1}{2}}} + ks_2^4 + e \frac{|s_2|^{\frac{3}{2}}}{1 + |s_2|^{\frac{1}{2}}} + \dots + ks_5^4 + e \frac{|s_5|^{\frac{3}{2}}}{1 + |s_5|^{\frac{1}{2}}} \right)
 \end{aligned}$$

It can be seen from the above formula that the $\dot{V} \leq 0$, so the control system is asymptotically stable.

4. Experimental simulation and analysis

4.1. Circuit implementation of the five-dimensional fractional-order chaotic system

In order to verify the dynamic behavior of the system (2), a nonlinear chaotic circuit is designed according to its mathematical model. When designing this nonlinear circuit, in order to better observe the state change diagram of the system and limit the system variables within the allowable range of circuit elements, the system equation is scaled without changing the nature of the system. The time scale transformation is performed as $\tau_0 = 100$, $\tau = \tau_0 t$, then the system (2) is transformed to the following form.

$$\begin{cases} \frac{d^x x}{dt^x} = 3000(y-x) + 100u + 200v - 500z \\ \frac{d^y y}{dt^y} = 1000x - 100xz + 1200y \\ \frac{d^z z}{dt^z} = 100xy - 300z - 100v - 400x \\ \frac{d^u u}{dt^u} = 100pxy + 100yz - 200u \\ \frac{d^v v}{dt^v} = 300y \end{cases} \quad (7)$$

According to Eq. (7), the circuit equation and circuit diagram can be designed. The circuit equation of the system is shown in Eq. (8):

$$\begin{cases} \frac{d^x x}{dt^x} = \frac{R_7}{C_x R_6} \left(\frac{y}{R_1} - \frac{x}{R_2} + \frac{u}{R_3} + \frac{v}{R_4} - \frac{z}{R_5} \right) \\ \frac{d^y y}{dt^y} = \frac{R_{11}}{C_y R_{12}} \left(\frac{x}{R_8} - \frac{xz}{R_9} + \frac{y}{R_{10}} \right) \\ \frac{d^z z}{dt^z} = \frac{R_{17}}{C_z R_{18}} \left(\frac{xy}{R_{13}} - \frac{z}{R_{14}} - \frac{v}{R_{15}} - \frac{x}{R_{16}} \right) \\ \frac{d^u u}{dt^u} = \frac{R_{22}}{C_u R_{23}} \left(\frac{xy}{R_{19}} + \frac{yz}{R_{20}} - \frac{u}{R_{21}} \right) \\ \frac{d^v v}{dt^v} = \frac{R_{24} y}{C_v R_{25} R_{26}} \end{cases} \quad (8)$$

If the value of the circuit elements in Eq. (8) is taken as follows:

$$\begin{aligned}
 R_i (i = 6, 8, 12, 18, 23, 25) &= 10 \text{ k}\Omega, \\
 R_i (i = 7, 8, 11, 17, 22, 24) &= 10 \text{ k}\Omega,
 \end{aligned}$$

$$\begin{aligned}
 R_{16} &= 2.5 \text{ k}\Omega, \quad R_i (i = 1, 2) = 0.33 \text{ k}\Omega, \\
 R_i (i = 3, 9, 13, 15, 20) &= 10 \text{ k}\Omega,
 \end{aligned}$$

$$\begin{aligned}
 R_i (i = 14, 25) &= 3.33 \text{ k}\Omega, \quad R_5 = 2 \text{ k}\Omega, \\
 R_i (i = 4, 21) &= 5 \text{ k}\Omega, \quad R_{10} = 0.83 \text{ k}\Omega,
 \end{aligned}$$

$$C_i (i = x, y, z, u, v) = 1 \text{ mF},$$

then the chaotic circuit is shown in Fig. 6.

By using MULTISIM 14.0 software to simulate the system circuit, the chaotic attractor and the x-dimensional time series are observed as shown in Fig. 7. Through the comparison, it can be seen that the designed chaotic circuit is consistent with the MATLAB analysis in Fig. 2.

4.2. Sliding mode control of the five-dimensional fractional-order chaotic systems

In order to improve the stability of the system (2), the sliding mode control is performed by Eq. (6) to make it quickly enter a predetermined motion state and maintain stability.

Setting parameters $x_e = \sin(2t)$, $y_e = 0.8 \sin(2t)$, $z_e = \sin(2t)$, $u_e = 3 \sin(2t)$, $v_e = 2 \sin(2t)$, $h = 0.0001$, $\varepsilon = 0.0001$, $c_1 = 100$. When the sliding mode control is added to the system at $t = 20s$, the simulation results are given as in Figs. 8, 9, 10, 11 and 12.

Figure 8 shows the x-dimensional time series and error response diagram with adding sliding mode control. It can be seen from Fig. 8 that the system is in an irregular oscillation state before 20 s, which indicates the system is unstable and in a state of chaotic motion. When the sliding mode control is added in 20 s, the system starts to track the set value x_e , thus a periodic motion state appears and the system reaches stability. Figure 8 also shows that after sliding mode control is added at 20 s, the error response curve quickly drops to around 0, and the system tends to be stable.

Figure 9 displays the y-dimensional time series and error response diagram with adding sliding mode control. Correspondingly, Figs. 10, Fig. 11 and Fig. 12 are the z-dimensional, u-dimensional curves and v-dimensional curves. According to all the above simulation results, it can be seen that after adding sliding mode control, the five dimensions of the chaos system can quickly reach the set stable state.

In Fig. 13, some projections of the controlled new five-dimensional fractional-order system are given. It also can be seen from Fig. 13 that after adding sliding mode control at 20 s, the system transforms from chaotic motion to periodic state, and the system quickly tracks the given reference value, which proves the good control effect of the sliding mode controller.

5. Conclusions

The dynamic characteristics of fractional-order chaotic system are more complex than those of integer-order system. Under certain conditions, chaos will do harm to the system. In order to study how to suppress chaos and control it to enter a predetermined state of motion and maintain stability quickly, a new five-dimensional fractional-order chaotic system was constructed and a new sliding mode controller was proposed in this paper. Firstly, the dynamic analysis was performed on the constructed five-dimensional fractional-order chaotic system through the 0–1 test. Then, a sliding mode controller was designed to realize the periodic control of the chaotic system in a stable state. And lastly, in order to verify the feasibility of the proposed method, circuit realization and control process simulation were performed on the five-dimensional fractional-order chaotic system, respectively. The simulation experimental results indicate that although the dynamic behavior is complex, the sliding mode controller has a good control effect on the five-dimensional fractional-order chaotic system.

Acknowledgements This work was supported by the Science and Technology Program of Hunan Province (No. 2019TP1014), the Educational Science Planning Key Project of Hunan Province (No. XJK19AGD007), the Normal University Teaching Reform Research Project of Hunan Province (No. [2019]291-630) and the Scientific Research Innovation Team of Hunan Institute of Science and Technology (No. 2019-TD-10).

References

- [1] O E Rössler *North-Holland*. **71** 6 (1979)
- [2] J Lü and G Chen *International Journal of Bifurcation and Chaos*. **12** 4620 (2002).
- [3] Y Z Liu, C S Lin and C S Jiang *Journal of University of Electronic Science and Technology of China*. **2** 235 (2008).
- [4] A K Alomari, M S M Noorani and R Nazar *Physica Scripta*. **81** 45005 (2010).
- [5] C L Li, J B Xiong and W Li *Optik - International Journal for Light and Electron Optics*. **125** 575 (2014)
- [6] J H Lu and G R Chen *International Journal of Bifurcation and Chaos*. **16** 775 (2006)
- [7] S M T Nezhad, M Nazari and E Gharavol *Electronics News-weekly*. **20** 700 (2016).
- [8] C B Li, J C Sprott, W Hu and Y J Xu *International Journal of Bifurcation and Chaos*. **27** 1607 (2017).
- [9] S Vaidyanathan, A Akgul, S Kaçar *Springer Berlin Heidelberg*. **133** 46 (2018)
- [10] H K Chen *Pergamon*. **23** 1245 (2005)
- [11] M P Aghababa *Nonlinear Dynamics*. **78** 2129 (2014)
- [12] M M Aziz and S F Al-Azzawi *Applied Mathematics*. **7** 292 (2016)
- [13] Z C Wei, A Akgul, U E Kocamaz *Chaos, Solitons and Fractals: the interdisciplinary journal of Nonlinear Science, and Nonequilibrium and Complex Phenomena*. **111** 157 (2018)
- [14] X Zhang, C B Li, Y D Chen, et al *Chaos, Solitons and Fractals: the interdisciplinary journal of Nonlinear Science, and Nonequilibrium and Complex Phenomena*. **139** (2020)
- [15] E Zambrano-Serrano, E Campos-Cantón and J M Muñoz-Pacheco *Nonlinear Dynamics*. **83** 1629 (2016)
- [16] R J Escalante-González, E Campos-Cantón and M Nicol *Chaos: An Interdisciplinary Journal of Nonlinear Science*. **27** (2017)
- [17] H E Gilardi-Velázquez and E Campos-Cantón *International Journal of Modern Physics C*. **29** 3 (2018).
- [18] M R Da, N A Kant, and F A Khanday *International Journal of Bifurcation and Chaos*. **27** 5 (2017)
- [19] K Li, J Cao, and J M He *Chaos*. **30** 3 (2020)
- [20] J F Chang, M L Hung, Y S Yang, et al *Pergamon* **37** 609 (2008)
- [21] U E Kocamaz, Y Uyaroglu and H Kizmaz *International Journal of Adaptive Control and Signal Processing*. **8** 1413 (2014).
- [22] S Vaidyanathan *International Journal of Chemtech Research*. **8** 25 (2015)
- [23] R Karthikeyan, K Anitha and K S Ashok *Nonlinear Dynamics*. **87** 2281 (2017).
- [24] H T Yau, C K Chen and C L Chen *International Journal of Bifurcation and Chaos*. **10** (2000)
- [25] C C Wang and J P Su *International Journal of Bifurcation and Chaos*. **13** 863 (2003)
- [26] A M Harb and A N Natsheh *International Journal of Modelling and Simulation*. **29** 1 (2009).
- [27] D Y Chen, Y X Liu, X Y Ma, et al *Nonlinear Dynamics*. **67** 893 (2012)
- [28] M Roohi, M H Khooban, Z Esfahani, et al *Transactions of the Institute of Measurement and Control* **41** 10 (2019)
- [29] G A Gottwald and I Melbourne *Proceedings of the Royal Society A: Mathematical, Physics and Engineering Sciences* **460** 603 (2004)

Publisher's Note Springer Nature remains neutral with regard to jurisdictional claims in published maps and institutional affiliations.